



Virginia Commonwealth University
VCU Scholars Compass

Theses and Dissertations

Graduate School

2014

High Speed Atomic Force Microscope Design Using DVD Optics

Thomas Carlson

Virginia Commonwealth University

Follow this and additional works at: <http://scholarscompass.vcu.edu/etd>

 Part of the [Physics Commons](#)

© The Author

Downloaded from

<http://scholarscompass.vcu.edu/etd/3427>

This Thesis is brought to you for free and open access by the Graduate School at VCU Scholars Compass. It has been accepted for inclusion in Theses and Dissertations by an authorized administrator of VCU Scholars Compass. For more information, please contact libcompass@vcu.edu.

High Speed Atomic Force Microscope Design Using DVD Optics

A thesis submitted in partial fulfillment of the requirements for the degree of Master of Science at Virginia Commonwealth University.

by

Thomas Beatty Carlson
Bachelors of Science, Physics, Virginia Commonwealth University 2012

Director: Dr. Jason Reed, Assistant Professor, Physics Department

Virginia Commonwealth University
Richmond, Virginia
May 2014

Acknowledgment

I wish to express my gratitude to several people. I would like to thank my wife, Angel for her undying support and faith in me. I wish to thank my children and my parents for their support and help without question. I wish to my advisor Dr. Jason Reed and my collaborator Dr. Loren Picco. I also wish to thank my committee members Dr. Marilyn Bishop and Dr. Christopher. Finally, I want to thank the entire VCU Physics Department for sharing their knowledge.

Table of Contents

I.	Introduction	
	1.1: About this study	2
II.	AFM	
	2.1: AFM background.....	4
	2.2: Specific applications	6
	2.3: Sources of noise in AFM.....	7
III.	Commercial OPU	
	3.1: Advantages of the OPU	10
	3.2: How the OPU works.....	11
	3.3: Powering the OPU	14
IV.	VCU test setup	
	4.1: Characterization of Noises in System Design	17
	4.2: Investigation of Noise.....	19
	4.3: Results showing thermally excited resonance peak.	20
V.	Imaging Results	
	5.1: Imaging of DNA samples	22
	5.2: Improvements to the imaging process	24
VI.	Conclusion.....	26
VII.	Bibliography	29

List of Figures

2.1-1: Standard AFM Setup	5
2.3-1: Example of thermal spectra of resonance peak for AFM cantilever.	8
3.2-1: Laser path through the OPU.....	11
3.2-2: Laser path through the OPU.....	13
3.2-3: S_{FE} versus defocus distance.....	14
3.3-1: Voltage divider circuit	15
3.3-2: Mounting setup for HSAFM	16
4.1-1: Bruker MSNL-10 scanning probe	17
4.1-2: FFT spectrum of the displacement or motion of the cantilever in the initial setup	18
4.2-1: FFT spectrum of the displacement or motion of the cantilever. The newer noise floor	
4.3-1: FFT spectrum of the displacement or motion of the cantilever in the current set up. Shows thermally excited resonance peak Design	21
4.3-2: Current System Setup	21
5.1-1 Topographic images of unidentified features formed on the surface of a mica substrate	23
5.1-2 Topographic images of the same sample as above showing additional unidentified features formed on the surface of a mica substrate.	24
5.2-1: Topographic images of features formed on the surface of a mica substrate.	25

List of Abbreviations

AFM:	Atomic Force Microscope/Microscopy
CD:	Compact Disk
DAQ:	Data Acquisition
DC:	Direct Current
DVD:	Digital Versatile Disk
FES:	Focus Error Signal
FFT:	Fast Fourier Transform
HSAFM:	High Speed Atomic Force Microscope/Microscopy
LD:	Laser Diode
LDC:	Laser Diode Controller
NI:	National Instruments
OPU:	Optical Pickup
PDIC:	Photo Diode Integrated Circuit
ROM:	Read Only Memory
VCM:	Voice Coil Motor
VDC:	Voltage Divider Circuit

Abstract

HIGH SPEED ATOMIC FORCE MICROSCOPE DESIGN USING DVD OPTICS

By Thomas Beatty Carlson, MS Applied Physics

A thesis submitted in partial fulfillment of the requirements for the degree of Master of Science at Virginia Commonwealth University.

Virginia Commonwealth University, 2014

Director: Dr. Jason Reed, Assistant Professor, Physics Department

We examine the design of a high speed atomic force microscope using an optical pickup from a commercially available compact disc/digital versatile disc drive. An investigation of the commercial optical pickup is done with the goal of determining how it can be used for dimensional measurements on nanometer scale. An evaluation of noise sources, imaging capabilities, and functionality is performed.

I. Introduction

1.1 About this study

This study is part of larger collaborative effort to develop a high speed atomic force microscope (HSAFM) using a commercial optical pickup (OPU) unit from a CD/DVD disk drive. This approach is being utilized in only two places throughout the world (Virginia Commonwealth University and University of Bristol). This project was performed under the direction of Dr. Jason Reed, Virginia Commonwealth University.

The AFM is a widely used tool in nano-science. Its purpose is to image and characterize surfaces on the nanometer scale. The biggest problem facing AFMs is slow scan speeds. In recent years scientists have begun to approach these problems, leading to the emerging field of high speed atomic force microscopy (HSAFM). A major advantage of HSAFM is the extremely fast operating speed. Using optics system contained within the Optical PickUp (OPU) from a commercial digital versatile disc (DVD) drive, a system could provide real time imaging, the opportunity for low cost (under \$10) and a compact size (approximately 40 x 50 x 12 mm). These features are extremely desirable because they are beneficial to the end user.

The goal of this project was to construct this system in our lab, investigate the workings of the various components, and evaluate noises in the system. We then determined the best options for optimization of functionality, noise reduction and image quality.

II. AFM

2.1 AFM Background

The Atomic Force Microscope (AFM) uses a cantilever with a sharp probe at its end to scan the surface of a given sample. In the AFM, the cantilever tip is brought into close proximity of a sample surface. Once the tip is in range, interatomic forces between the tip and surface result in a deflection of the cantilever according to Hooke's Law (Binnig & Quate, 1986, Vol. 56). Typical spring constants range between 0.001 to 100 N/m, and deflections of the cantilever can range from microns to fractions of a nanometer. Typical forces between the cantilever and sample can range from 10^{-11} N to 10^{-6} N. For comparison, the interaction between two covalently bonded atoms is of the order of 10^{-9} N at separations of an angstrom. Therefore, non-destructive imaging is possible. (*Atomic Force Microscopy, E. Meyer. Progress in Surface Science, Vol. 41, pp. 3-49*)

AFM images are formed by scanning a sample relative to the probing tip and then measuring the deflection of the cantilever (in the vertical or z direction), as a function of the lateral positions (x and y). At small separations, of the order of an angstrom, the tip of the cantilever is in contact with the sample. In this mode, repulsion forces allow the surface topography to be traced with high

resolution. Atomic resolution can be obtained under ideal conditions (Meyer, 1992, Vol. 41).

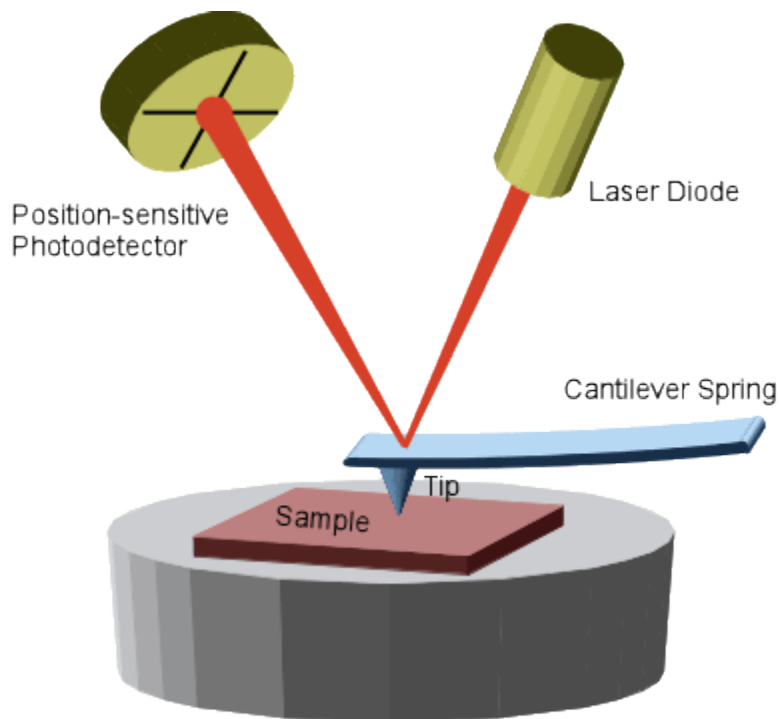


FIGURE 2.1-1: Standard AFM Setup (Uni-Greifswald).

Currently, the most common method for measuring the deflection of the cantilever is optical beam deflection. As the cantilever flexes, the light from the laser is reflected onto the split photo-diode. By measuring the difference signal, changes in the bending of the cantilever can be measured. The adoption of this method has been successful, because the sensitivity (better than 0.1 nm) is sufficient to produce quality imaging.

Recently it has been shown that using the optical pickup from a commercial CD/DVD ROM drive is sufficiently sensitive for detecting deflections of a cantilever tip down to an atomic step (HWU, Kuang-Yuh HUANG, & HWANG, 2006, Vol. 45, No. 3B). This implies that under certain conditions the

optical system in the CD/DVD pickup has a sensitivity level comparable to that of the beam deflection method in terms of the displacement measurement of the cantilever.

2.2 Specific Applications

A primary concern in our lab is the investigation of biological materials such as DNA and other molecular complexes. AFM is a useful technique for observing DNA. As an example, the AFM can be used to image DNA molecules and DNA–enzyme interactions. AFM images of static DNA–enzyme interactions give information about enzyme locations on DNA (Hansma, 1996). Measured heights of DNA in AFM have been reported to vary from 0.5 to 1.9 nm in air. Thus we wanted to make our system sensitive enough to detect variations in height on this scale.

High speed techniques allow for the possibility of exploring molecular and cellular dynamics in real time. Time resolution is critical factor limiting the use of AFM in live cell studies. Recently scientists have used AFM provide images of the chemical bonds between atoms. In some situations, imaging can depict how a molecule's structure changes during a reaction (Sanders, 2013).

Another possible area of interest will be nanoparticles. Particles on the nanometer scale have unique optical, electronic, and structural properties that are not available in either isolated molecules or bulk solids. Nanoparticles are

also becoming increasingly important in many areas such as biomedical applications (A Rao, 2007). Our setup should allow us to visualize individual particles and groups of particles.

2.3 Noise sources in AFM

If the OPU is to be used effectively as a detection system, noise sources must be considered. A primary source of AFM noise results from optical shot noise. Optical shot noise is due to random fluctuations in optical phase due to the quantization of light into wave packets (Daw, 2001). Shot noise sets the fundamental limit of detection of the optical beam deflection method and its reduction plays a primary role in enabling atomic resolution imaging (Aleksander Labuda, 2012). Radiation pressure of the laser on the cantilever was also considered. AFM experiments using this setup are performed at the resonance frequency of the thermally excited cantilever, thus the thermal noise of the cantilever ($\sim 10^{-12} \frac{m}{\sqrt{Hz}}$) is greater than noise originating from the detector or from back-action forces, such as radiation pressure ($\sim 10^{-15} \frac{m}{\sqrt{Hz}}$) (Smith, 1994). Noise in AFM systems can also arise in part due to thermal Brownian vibration of the cantilever. Brownian motion is random motion that results from collisions with atoms or molecules in a surrounding gas or liquid. The noise in the our detection system must be less than that of the thermal noise in order to obtain thermal noise limited performance. Our detection system must ensure that the noise floor is sufficiently low as to allow us to observe the thermally excited resonance peak

of the cantilever, an example can be seen in figure 2.3-1. A high noise floor will conceal the presence of resonance peak and make quality measurements impossible.

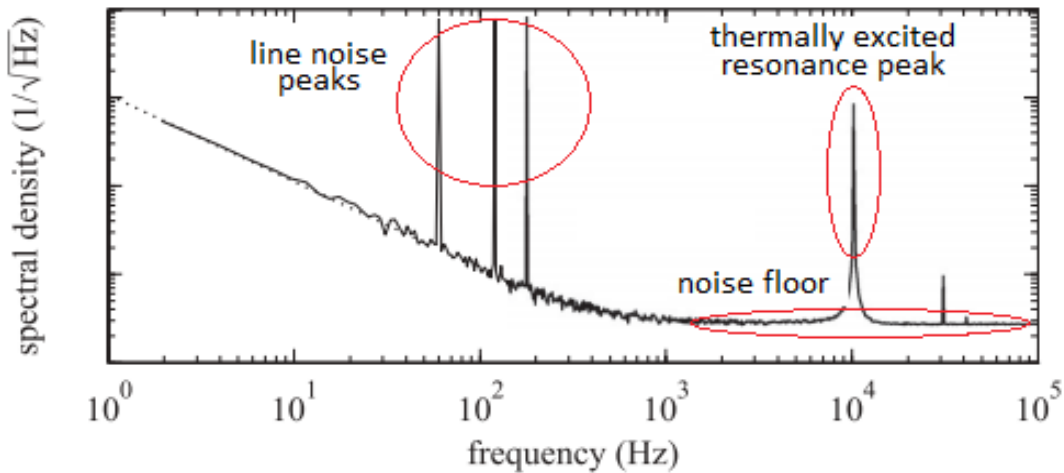


FIGURE 2.3-1: Example of thermal spectra showing the resonance peak for the AFM cantilever.

Another source of noise in systems that use optical detection is known as intensity noise. It is in part the result of quantum noise associated with laser gain and resonator losses. Intensity noise also results from technical noise sources such as excess noise of the power source, vibrations of the resonator, and thermal fluctuations in the gain medium. The resulting intensity noise often becomes weaker at higher power. In most cases, the lowest possible intensity noise level for laser beams results in a higher shot noise (Paschotta, 2008).

Custom electronics are needed to power portions of the OPU. Electronic and electrical noises were also considered in this setup. As is the case with optical systems, noise is ever-present in electronics. Electronic or circuit noise is,

in large part, the result of two processes. The first produces thermal noise effects. Thermal noise, also known as Johnson noise is due to the result of electrons moving about in a resistive material. The second is well known as shot noise. Shot noise is due to random fluctuations in direct current circuits. As current flows through a device, there are random fluctuations in the transit time of electrons. Current flow also causes the random emission of electrons from material surfaces. Both of these factors contribute to the effect of shot noise. It is noted that thermal noise is generated in active and passive components, while shot noise comes only from active components, such as a DC power supply (Vergers, 1987).

Though it is possible for us to measure the overall RMS noise from our electronic circuitry, we cannot predict all of the sources of noise. Improper grounding of circuits and other equipment plugged into the same circuit can pose potential noise problems. Using quality components can be an effective means of reducing circuit noise. Many components are made of materials best known for their low noise qualities. Shielding our setup, electrically isolating our setup from other laboratory equipment, and reducing wire length, a source of electronic cross-coupling, can all be effective ways to reduce noise.

Micro and nano-scale measurement experiments can be severely hampered by small vibrations. For example, many optical applications require a laser with a spot size of just a few microns. If the position of this spot is critical to system performance, such as its position on the tip of a cantilever, then vibrations with amplitudes in the micron range can inevitably cause experimental

failure. In our laboratory environment vibrations may be the result of equipment such as computers, power supplies, and fans. Thus, it was necessary to vibrationally isolate our system using commercially available equipment.

III. The commercial OPU

3.1 Advantages of the OPU in AFM deflection sensing

Standard AFM in systems can be designed to run at high speeds; however, they require electronics designed to operate at high bandwidths with low noise. Such equipment can be a major operating cost at \$50,000 and above. The OPU from a CD/DVD disc drive is the commercially designed to operate at speeds in the MHz range. Wide availability and low cost (under \$10) of the OPU provide an attractive alternative to much of the equipment need to develop a HSAFM system. Commercial CD/DVD pickups are also compact, lightweight, and reliable, and thus may greatly simplify the design of HSAFM systems.

Another advantage of the OPU in HSAFM setups is that the astigmatic detection system (discussed in section 3.2) is used to make quantitative measurement of the height displacement of the cantilever (E.-T. Hwu, 2007). In the standard optical beam deflection detection system, angular changes are measured and assumed to be due to only to the bending of the cantilever below its resonance frequency. This assumption is not always correct. In high-speed AFMs, the cantilever often has oscillations at the second, third and even higher harmonics (O. D. Payton, 2012). This adds extra bending to the cantilever which

gets incorrectly interpreted as height changes from the surface. A common problem induced by multiple probe effects is the shadowing or multiplication of small structures produced (Dufrêne, 2002).

3.2 How the OPU works

The commercial OPU is comprised of several optical and electronic components that are manufactured in a single casing. In this set up we use the *Phillips OPU66.50 D* Optical Pickup Unit (Royal Phillips Electronics, 2005). The laser diode provides light at a wavelength of 658 nm. A schematic of the light path in the OPU can be seen in figure 3.2-1.

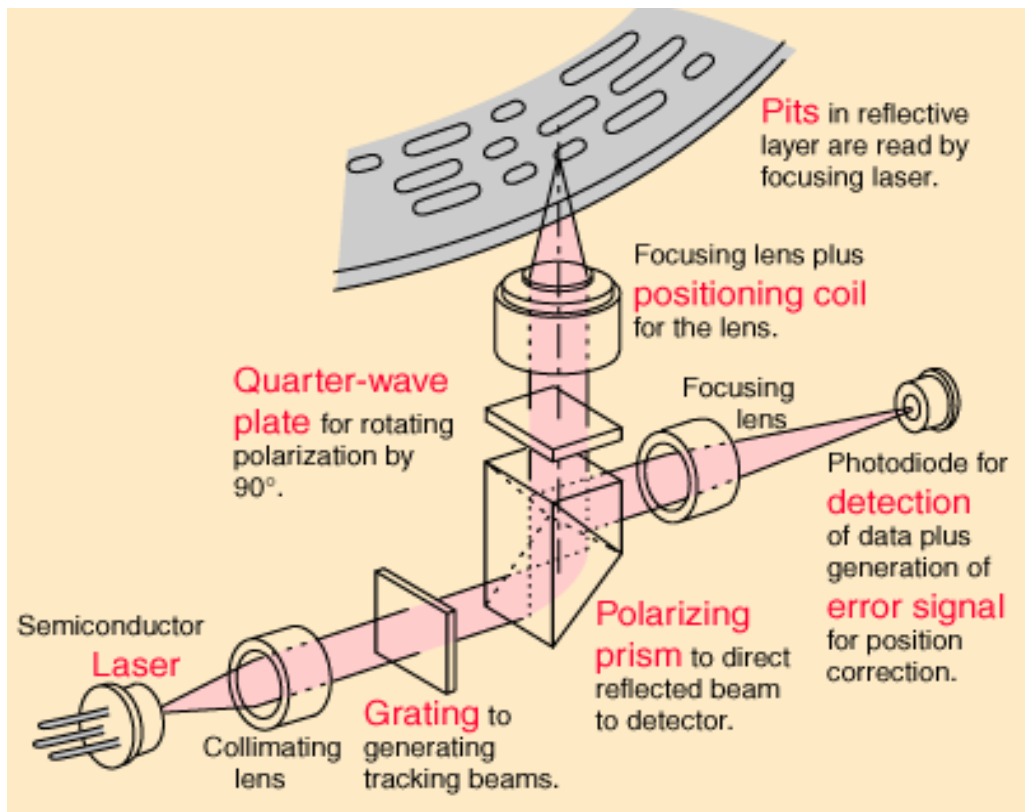


FIGURE 3.2-1: Laser path through the OPU (Science Blogs, 2012)

As light leaves the laser diode it immediately enters a collimating lens, converting the Gaussian profile of the beam into a uniform one. Processing optical data requires a collimated uniform laser beam that maintains the phase of the incident wave front. The collimating lens is made of neutral density glass to produce the Gaussian absorption profile so that the output beam becomes uniform (Chang-Yuan Han, 1983, Vol. 22, No. 22).

Once the beam has been made uniform, it passes through a diffraction grating that is used to split the main beam into a central beam for reading information and side beams for tracking disc position and keep the main beam in place. We remove the diffraction grating, as it is not necessary in our application. This gives main beam a more powerful signal at lower driving currents.

Laser light then passes through a polarizing beam splitter, also known as a polarizing prism. This divides the incident light beam into a reflected beam and a transmitted beam. The beam splitter is also used to combine two incoming beams of light (Saleh & Teich, 2012). Additionally, the polarizing beam splitter provides the means to extract polarized light from un-polarized light. To do this two prisms of uniaxial anisotropic material are cemented together. When light enters an anisotropic crystal, the ordinary and extraordinary waves refract at different angles, causing separation. At the interface, a dielectric film is used to modify the reflective properties of the surface by exploiting the interference of reflections from multiple optical interfaces (Paschotta, 2008).

A quarter wave plate also known as a $\pi/4$ wave retarder, then serves to convert the light into circularly polarized light. The laser is then focused by a lens to a single point, seen in figure 3.2-2. The focus distance of the OPU is 2.75mm.

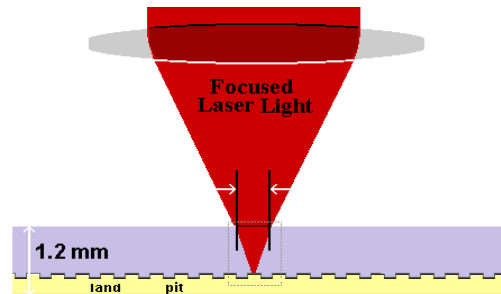


FIGURE 3.2-2: Laser light focused on the disc surface (Science Blogs, 2012).

In the return path, light reflected from the surface passes back through the lens and the quarter wave plate where it is now 90 degrees out of phase with the incoming light. This keeps the incoming and outgoing light beams from interfering with each other. The detection of the focusing condition of the laser beam on the optical disk adopts the astigmatic method, which uses a cylindrical lens as a beam-shaping device (F. Quercioli, 1997). When the laser beams are perfectly focused on the disk surface, the laser spot is circular, and evenly centered on the four photo-detectors (A–D) as seen in Figure 3.2-3. When the disk surface is slightly higher or lower than the focus of the laser beam, the laser spot on the central quadrant sensors becomes more elongated. The shape change of the laser spot on the photo-detector is detected by the Focus Error Signal (FES).

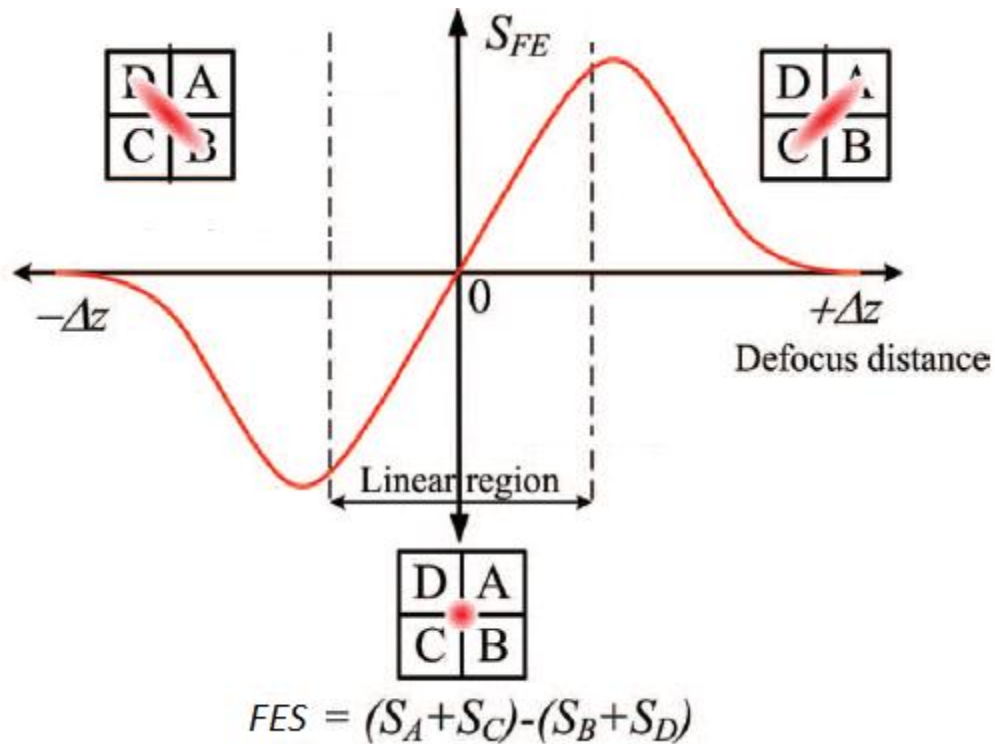


FIGURE 3.2-3: *FES* versus defocus distance. The corresponding light spot projected on the photodiode is shown at three different defocus distances. (HWU, Kuang-Yuh HUANG, & HWANG, 2006, Vol. 45, No. 3B)

The FES returns linear displacement information from the disk, which is given by the following equation:

$$FES = (S_A + S_C) - (S_B + S_D).$$

where S_A , S_B , S_C , and S_D are the output voltage of each quadrant respectively, as shown in Figure 3.2-3. Plotting the FES as the laser passes through the focus region results in an S-shaped curve as seen in the figure. The linear region of this S-curve allows us to determine displacement of the cantilever as a linear function of the FES. The detectable displacement range of the *Phillips OPU66.50* D is $6.5 \mu\text{m}$. The focus point is $\pm 3.25 \mu\text{m}$ about the center of the beam

3.3 Utilizing the OPU

To use the OPU for measurement we needed to provide power and be able to read back the voltage signals from it. To power the laser, we use the *Thorlabs LDC 201 C* laser diode controller. The FES is provided by a Photo-Diode Integrated Circuit (PDIC) that requires voltage levels of 2.1 V, 2.5 V, and 5 V. The 5 V signal powers the PDIC, 2.1 V is used as a reference voltage for the photodiode, 2.5 V powers the various gain settings. To do this we have designed a voltage dividing circuit capable of taking an input voltage and outputting the necessary voltage levels. The Agilent U8001A regulated DC power supply is used to supply to power the circuit. A diagram of the circuit used is shown in Figure 3.3-1.

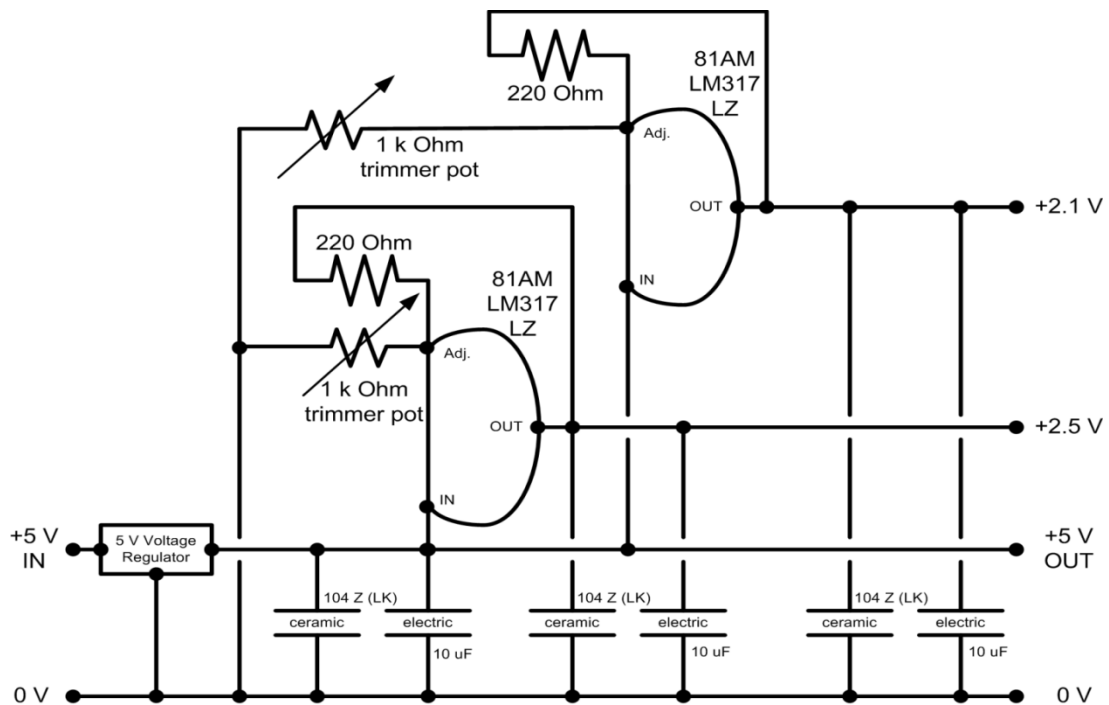


FIGURE 3.3-1: Voltage divider circuit (Payton, 2014).

The FES returned by the PDIC is read by a National Instruments (NI) USB-6259, a Data Acquisition (DAQ) interface with NI *LabView* Software. The DAQ is capable of reading input signals up to 1.25 MHz which will allow us to collect data at the desired speeds. *Labview* allows us to create the necessary Virtual Instruments (VI) for gathering data and displaying image information.

The OPU is mounted onto a manual x-y-z micrometer stage such that the laser is directed straight down, as seen in figure 3.3-2. This gives us the freedom to position the laser spot directly over top of the cantilever. The cantilever is fixed to a stationary, transparent polycarbonate film. The sample sits on an x-y scanning stage that is have fixed to a z-stage, allowing the scanning stage to engage the cantilever. The scanning stage is capable of moving at high frequencies in the x and y directions, allowing a sample to be imaged in real time. The entire setup is mounted on a breadboard with rubber feet, and sits atop a vibration isolation table.

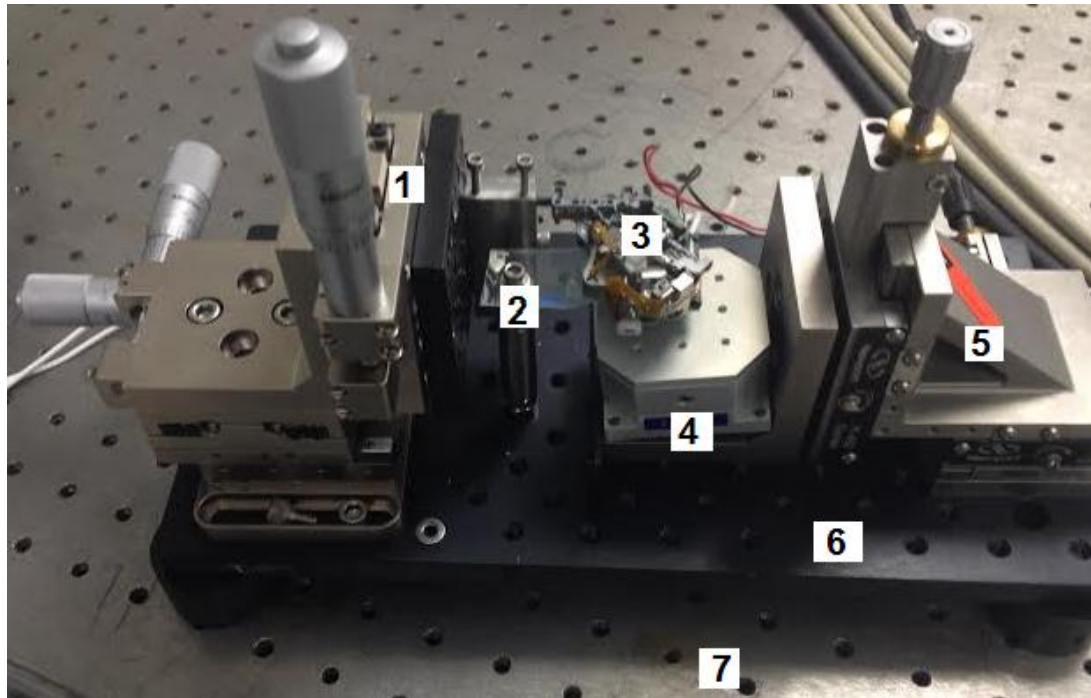


FIGURE 3.3-2: Mounting setup for HSAFM. 1) x-y-z positioning stage 2) cantilever and holder 3) OPU 4) x-y scanning stage 5) x-z positioning stage 6) 6" x 12" ground isolating breadboard 7) vibration isolation table.

IV. VCU test setup

4.1 Evaluation of System Noise

The first goal of the HSAFM setup is detection of the thermally excited resonance peak of the cantilever. We used the Bruker MSNL-10 scanning probe. The MSNL-10 contains six cantilevers with varying degrees of force constants, ranging from 0.01 N/m to 0.6 N/m and resonant frequencies that range from 7 kHz up to 125 kHz. The back of the cantilever is coated with reflective gold, which returns a high percentage of the incident light. Cantilever “C” was chosen for measurement of the thermal peak. Its resonance frequency is 7 kHz and the spring constant is 0.01 N/m. The thermally excited amplitude of the cantilever motion was measured to be 2 nm using a *Polytec OFV-5000* laser Doppler vibrometer.

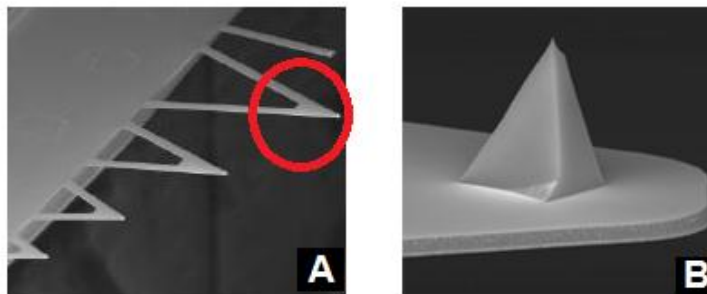


FIGURE 4.1-1: Bruker MSNL-10 scanning probe (A) cantilever “C,” 305 μm long and 17 μm wide at its end (B) tip radius is nominally 2 nm (Bruker Corporation).

The initial set up and testing did not yield the desired results. A review of the Fast Fourier Transform (FFT) motion spectrum revealed a higher than desired noise floor and a high number of frequency spikes, seen in figure 4.1-2. The strength of the FES was also observed to be too small at 20 mV peak-to-peak vs. the expected 200 mV peak to peak signal.

Issues related to noise were hypothesized to be the result of several factors, the first of which is electrical noise inherent in the building that houses our laboratory. Considerable crosstalk was found between our system and other electronic equipment in close proximity. A weak signal can arise from poor reflectivity. Thus the transparency of the polycarbonate film on which the cantilever was mounted was questioned. Laser noise was also considered as a possible factor. A highly unstable resonance peak was observed with the LDC current set at 72 mA, near the laser diode maximum current rating of 80mA. The spectral noise floor increased rapidly when LDC currents moved above 64 mA.

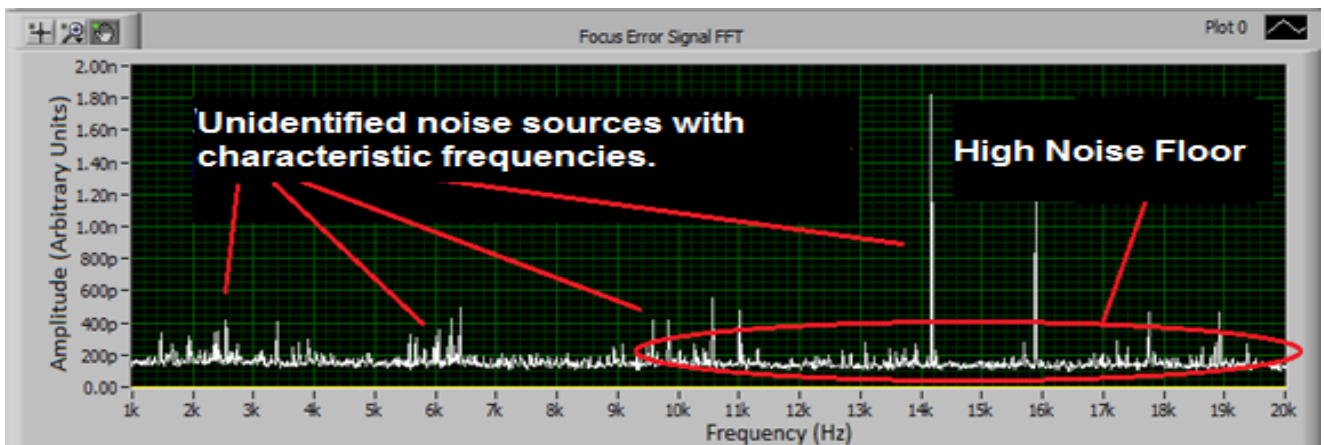


FIGURE 4.1-2: FFT spectrum of the displacement or motion of the cantilever in the initial setup showing undesired noises and a high noise floor.

4.2 Mitigation of Noise sources

In an effort to mitigate the effects of noise, several strategies were employed. Equipment and wiring was isolated from other electronic equipment. A line conditioner was used to reduce noise present in the building electrical supply. Additionally, the use of battery power in the VDC reduced electronic shot noises attributed to the regulated DC power supply. To increase reflectivity, the polycarbonate film was replaced, and the new film cleaned with an ethanol solution to improve transparency. The FES output of the OPU has been shown to suffer from serious signal drift problems (Hwu, 2012). Due to temperature fluctuation of the ambient environment, signal drift can be thousands of nanometers right after the optical head is switched on; thus the OPU was allowed warm up for at least 10 minutes after powering on. To reduce optical intensity noise and stabilize the laser output, the LDC current was set to 60 mA, 70% of the maximum operating current.

These methods reduced the overall noise floor from $10 \times 10^{-9} \frac{m}{\sqrt{Hz}}$ to $2 \times 10^{-9} \frac{m}{\sqrt{Hz}}$, and yielded a slight increase of the peak to peak voltage of the S-curve (refer to figure 3.2-3) from 20 mV to 40 mV. The results can be seen in figure 4.2-1.

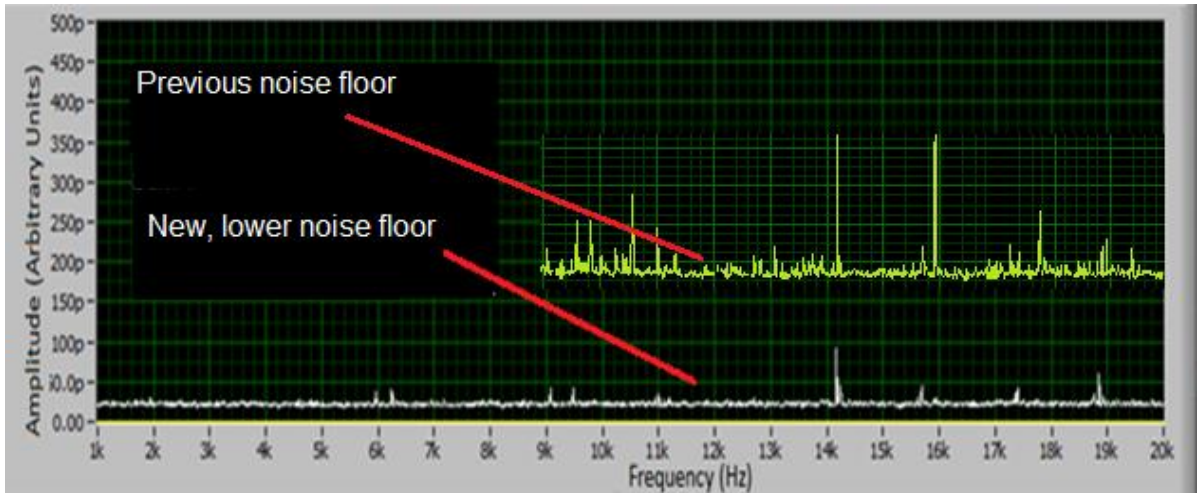


FIGURE 4.2-1: FFT spectrum of the displacement or motion of the cantilever. The newer noise floor is below initial noise floor levels (superimposed to show improvements).

Because we were not able to see the thermally excited resonance peak after the initial improvements, further mitigation was required. The use of battery power for the DAQ revealed a faulty DAQ power supply, which was replaced. This led to an orders of magnitude reduction in the noise floor from $2 \times 10^{-9} \frac{m}{\sqrt{Hz}}$ to $100 \times 10^{-12} \frac{m}{\sqrt{Hz}}$. The FES signal was dramatically improved. The peak to peak voltage of the S-curve now spanned 280mV, vs. 40 mV previously. This is in the expected range. In addition, we observed the elimination of most of the unidentified noises with characteristic frequencies

4.3: Results showing thermally-excited cantilever resonance peak

As a result of these improvements, we were ultimately able to resolve the thermally excited resonance peak. The thermal noise peak of the cantilever was detected at the expected normal resonance frequency of 7 kHz. The results can be seen in Figure 4.3-1 along with the initial noise floor level, the noise floor levels after initial improvements, and a the low noise floor achieved in the final setup.

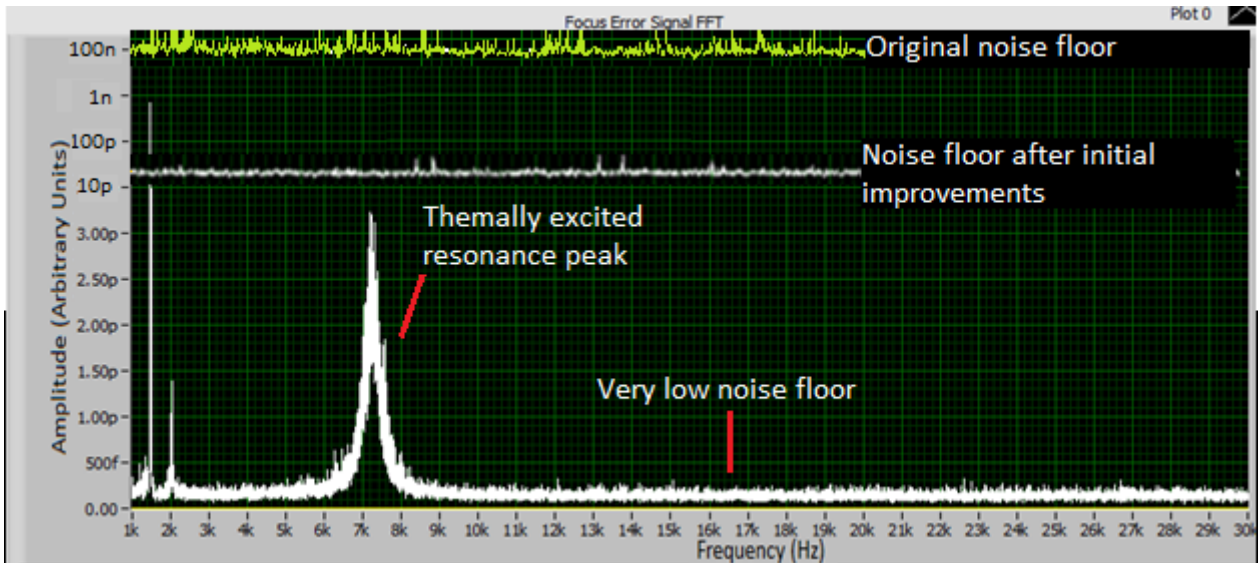


FIGURE 4.3-1: FFT spectrum of the displacement or motion of the cantilever in the current set up. Shows thermally excited resonance peak at the expected frequency of 7 kHz and a low noise floor. The upper half of the y-axis, above 3.00p, has been logarithmically scaled to show noise floor improvements from the initial setup

A picture of the current system under operation can be seen in figure 4.3-2. A computer with *NI Labview* software interprets signals from the DAQ. Electronic equipment is used to power the OPU and control the scanning stage. An oscilloscope is used to monitor the scanning stage position.

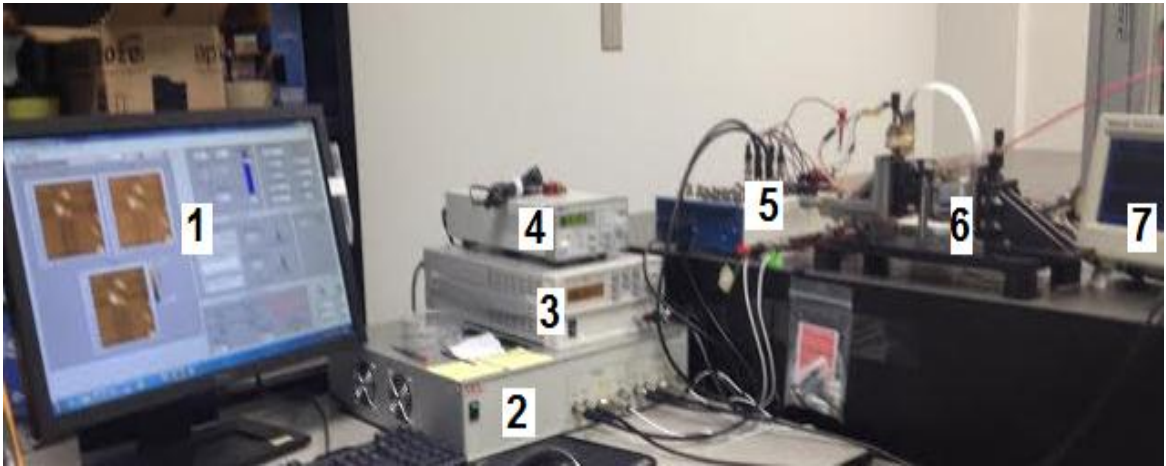


FIGURE 4.3-2: Current System Setup (1) Computer with NI Labview software. (2) Scanning stage controller. (3) DC power supply for VDC. (4) Laser diode driver. (5) DAQ (6) Microscope (7) Oscilloscope

V. Imaging Results

5.1 Imaging of DNA samples

To perform imaging using the HSAFM system, custom VIs are used to acquire deflection signals in a continuous time series. Images based on the information from the deflection signal are then displayed on screen. Because biological materials are an area of interest in our lab, samples of DNA are prepared for imaging. Samples are deposited on MgCl_2 -derivatized mica substrates by fluid shear flow and washed three times with purified water before being blown dry for 30 seconds (Jason Reed, 2012). The sample is set atop a Mad City Labs HS2 x-y nano-positioning scanning stage (Mad City Labs Inc., 2014) operated in closed loop mode. The fast scan direction (parallel to cantilever) is set to a frequency of 100 Hz. Initial data sampling rates were set at 200 kHz, more than sufficient for collecting data.

Initial imaging using the current system was able to detect aperiodic features on the surface of the sample. Figure 5.1-1 shows the topographic images of features formed on the surface of the sample during its fabrication. These are most likely salt crystals formed during sample deposition of DNA from

a dilute salt solution. Some salt and impurities bind to the mica and are not washed off. The same sample has been imaged with other AFMs in our lab and the particles appear similar in shape. The scanning stage amplitudes of 3 V and 6 V correspond to a scan area of 3 and 6 microns in (a) and (b) respectively. Diameters range from 100 to 500 nm with the OPU, currently. The height is not calibrated, and the height can only be estimated based on the size of these objects as seen on in other AFM images.

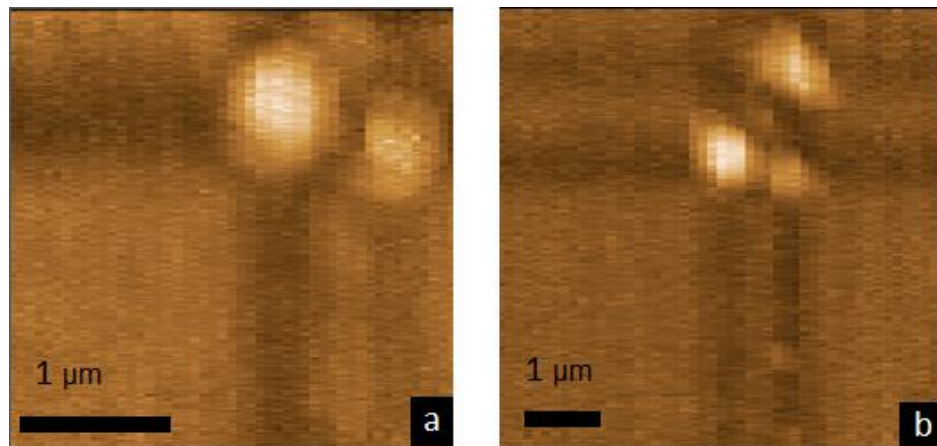


FIGURE 5.1-1 Topographic images of features formed on the surface of a mica substrate. (a) Surface feature resolved at a scan size of 3 microns (b) Same feature resolved in a scan area of 6 microns. Images contain 50 lines of resolution at 1000 pixels per line.

The dark patches seen around the objects are artifacts of bad fitting in the image flattening algorithms, which use polynomial line fitting (S. A. Tsiftaris, 2008). This can introduce a non-existent valley like deviation of the background.

The surface was further scanned for DNA. However, only additional salt crystals were found, seen in figure 5.1-1. In both cases, smaller scan sizes increased the size of the feature on the viewing screen and larger scan sizes

decreased the size of the same feature, confirming that imaging is actually occurring.

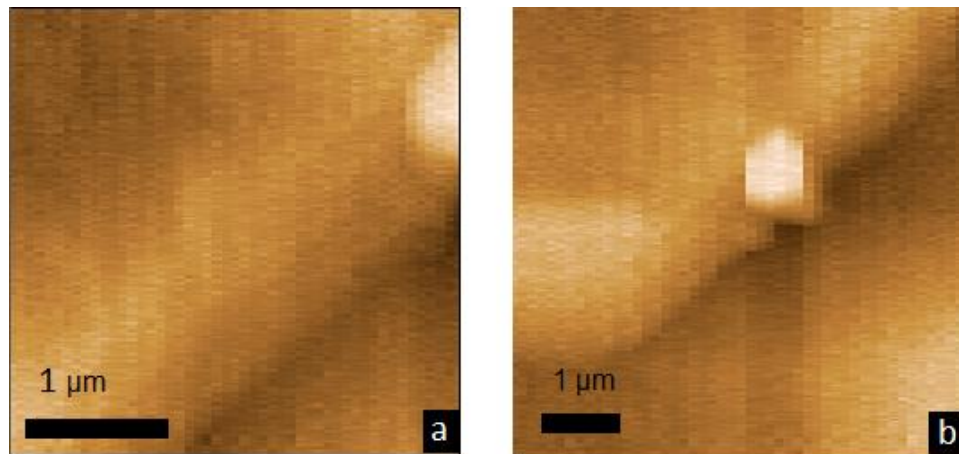


FIGURE 5.1-2 Topographic images of the same sample as above showing additional features formed on the surface of a mica substrate.

5.2 Improvements in the imaging process

Initial images confirmed that imaging was taking place. However, the quality was insufficient and needed to be improved to image DNA on the surface of the sample. To produce an image, analog signals provided to the computer by the DAQ produce discrete scan lines. Each scan line is divided into discrete pixels for image processing. The ordering of pixels by rows is known as raster order, or raster scan order. There are more pixels per line in the fast scan direction than there are lines, and thus the resolution is higher in the fast scan direction, and the pixels are not square. The horizontal resolution can be improved by increasing the sampling rate of the cantilever detection signal, thus increasing the number of detected height changes over the course of the scan

line. The vertical resolution of the image can be increased by increasing the number of scan lines in the image.

The number of pixels per line was increased from 1000 to 2000, and the number of lines of resolution from 50 to 125. The sampling rate of the cantilever deflection signal was increased from 200 kHz to 1 MHz. A new sample was also prepared in same manner as the previous sample. A scan of several regions of the new sample showed improved image quality, evidenced by resolution of finer structured details in surface-bound salt crystals. The amplitude of the scanning stage was set to 6 V, corresponding to a scan area of 6 microns. The two images below show features of relatively high spatial frequency, which indicates good quality scanning based on our observations with these samples on other AFMs. However we were ultimately unable to identify DNA using these settings with our current setup.

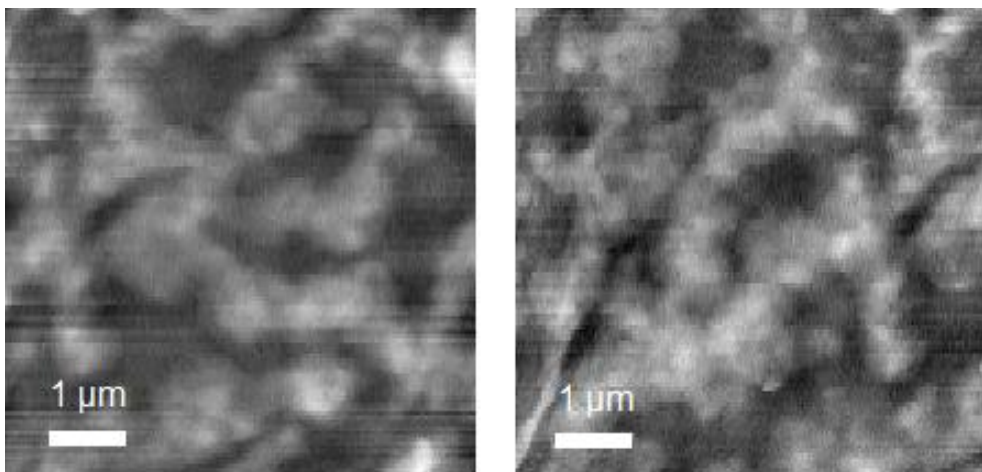


FIGURE 5.2-1: Topographic images of features formed on the surface of a mica substrate. Similar features were resolved in a separate scan areas, both 6 microns. Images contain 125 lines of resolution at 2000 pixels per line.

VI. Conclusion

We have demonstrated the capability of the CD/DVD OPU to detect the vertical cantilever displacement in a HSAFM system. The imaging of sub-micron sized nano-particles was achieved. Using the current setup the HSAFM system using DVD optics provides an low cost option that is practical for applications involving near molecular sized objects.

The HSAFM we have developed is capable of detecting nanoparticles, but not yet capable of resolving DNA on the surface of our samples. Further advancements could be made to the system in an effort resolve smaller feature sizes. The salt crystals that appear in our images are known to be only slightly taller than the DNA (0.06 nm). Comparison of the noise spectrum of our system with that of other HSAFM systems will show how much further work is needed to match the performance of other systems.

Image processing techniques could be used to improve image quality. One technique that has been shown to remove common image artifacts is the use of notch filters. (O. D. Payton, 2012). Once a noise peak present in the of the deflection signal data has been determined, it is possible to remove specific

contributions made by that frequency by applying a notch filter at the resonance frequency. This method decouples surface features from higher-mode oscillations of the cantilever and enables cantilever-induced noise sources to be filtered out. Image averaging algorithms are another image processing technique that can be used to remove random noise from a series of images. Random fluctuations above and below actual image data gradually even out if a sample area is averaged over time series images.

System functionality could be improved by taking advantage of the Voice Coil Motors (VCM) inside the OPU (Hwu, 2012). Compared to the manually operated micro-positioning stages currently used for OPU alignment, control of the laser spot can be performed more precisely by using the z and x axis actuators of the VCM. Focusing can be performed in the z direction, which has a range of motion $\pm 550 \mu\text{m}$. Positioning in the x direction offers a motion range of $\pm 400 \mu\text{m}$. The VCM has a sensitivity of 1.11 mm/V and can be precisely controlled by using a DC signal.

System functionality could further be improved by adding the capability of tapping mode. Our system currently operates in contact mode, meaning that the tip is kept in constant contact with the surface. During the scanning process the tip to sample force interactions of the order of 10^{-8} N can be enough to deform some biological materials. Contact mode also can have the tendency to sweep away weakly immobilized objects. An alternative to contact mode is found in tapping mode, in which the cantilever is oscillated vertically while scanning occurs. This reduces the lateral frictional forces that can apply to the sample

during contact mode. Tapping mode would be advantageous for imaging biological materials because of the force interaction between the cantilever tip and the sample is less than that of contact mode, of the order of 10^{-10} N, decreasing the likelihood of damage to the sample (P. K. Hansma, 1994).

VII. Bibliography

- A Rao, M. S. (2007). Characterization of nanoparticles using Atomic Force Microscopy. *Journal of Physics*, 971-976.
- Aleksander Labuda, M. L. (2012). Stochastic noise in atomic force microscopy. *Physical Review*.
- Binning, G., & Quate, C. F. (1986, Vol. 56). Atomic Force Microscope. *Physical Review Letters*, 930-933.
- Bruker Corporation. (n.d.). *Bruker AFM probes*. Retrieved May 1, 2014, from Bruker: <https://www.brukerafmprobes.com/Product.aspx?ProductID=3710>
- Chang-Yuan Han, Y. I. (1983, Vol. 22, No. 22). Reshaping Collimated Laser Beams with Gaussian Profiles to Uniform Profiles. *Applied Optics*.
- Daw, E. (2001, August). *An Introduction to Shot Noise in Laser Beams*. Retrieved February 2014, from <http://ligo.phys.lsu.edu/edaw/homepage/talks/shot.pdf>
- Dufrêne, Y. F. (2002). Atomic Force Microscopy, a Powerful Tool in Microbiology. *Journal of Bacteriology*, 5205-5213.
- E.-T. Hwu, S.-K. H.-W.-S. (2007). Simultaneous detection of translational and angular displacements of micromachined elements. *Applied Physics Letters*, 91, 221908.
- F. Quercioli, A. M. (1997). *Correlation optical velocimetry*. The Optical Society.
- Hansma, R. K. (1996). Atomic force microscopy of long and short double-stranded, single-stranded and triple-stranded nucleic acids. *Nucleic Acids Research*, pp. 713-720.

- Hwu. (2012). Anti-drift and auto-alignment mechanism for an astigmatic atomic force microscope system based on a digital versatile disk optical head. *American Institute of Physics, Review of Scientific Instrument*.
- HWU, E.-T., Kuang-Yuh HUANG, S.-K. H., & HWANG, a. I.-S. (2006, Vol. 45, No. 3B). Measurement of Cantilever Displacement Using a Compact Disk/Digital Versatile Disk Pickup Head. *Japanese Journal of Applied Physics*, 2368-2371.
- Jason Reed, 1. C.-L. (2012). Identifying individual DNA species in a complex mixture by precisely measuring the spacing between nicking restriction enzymes with atomic force microscope. *Journal of the Royal Society Interface*, 9 74 2341-2350.
- Mad City Labs Inc. (2014). *Nano-HS series*. Retrieved May 2014, from Mad City Labs: <http://www.madcitylabs.com/nanohssseries.html>
- Meyer, E. (1992, Vol. 41). Atomic Force Microscopy. *Progress in Surface Science*, 3-49.
- O. D. Payton, L. P. (2012). Improving the signal-to-noise ratio of high-speed contact mode atomic force microscopy. *Review of Scientific Instruments*, 83, 083710.
- P. K. Hansma, J. P. (1994). Tapping mode atomic force microscopy in liquids. *Applied Physics Letters*, 64, 1738 .
- Paschotta, D. R. (2008). *Encyclopedia of Laser Physics and Technology*. Wiley & Sons, Inc.
- Payton, O. D. (2014). *Voltage Divide Circuit*.
- Royal Phillips Electronics. (2005). *OPU66.50 D Optical Pickup Unit for DVD +R/RW, -R/RW, +R DL Data sheet*. Royal Phillips Electronics.
- S. A. Tsiftaris, J. Z. (2008). *AUTOMATED LINE FLATTENING OF ATOMIC FORCE MICROSCOPY IMAGES*. Retrieved May 2014, from http://users.eecs.northwestern.edu/~jzu850/papers_bib/tsiftaris08icip.pdf
- Saleh, B. W., & Teich, M. C. (2012). *Fundamentals of Photonics; 2nd Edition*. John Wiley & Sons Inc. .
- Sanders, R. (2013, May). *Scientists capture first images of molecules before and after reaction*. Retrieved May 1, 2014, from UC Berkeley News Center: <http://newscenter.berkeley.edu/2013/05/30/scientists-capture-first-images-of-molecules-before-and-after-reaction/>

Science Blogs. (2012, April). *Science Blogs*. Retrieved March 2014, from Science Blogs: <http://scienceblogs.com/principles/wp-content/blogs.dir/467/files/2012/04/i-2c6394b95db042cdf484322b78cfba9d-cdplay.gif>

Smith, D. P. (1994). *Limits of Force Microscopy*. IBM Research Division.

Uni-Greifswald, B. (n.d.). *Biophysik Uni-Greifswald*. Retrieved April 2014, from Biophysik Uni-Greifswald: http://www3.physik.uni-greifswald.de/method/afm/AFM_laser.gif

Vergers, C. A. (1987). *Handbook of Electrical Noise Measurement and Technology, 2nd Edition*. Blue Ridge Summit, PA: TAP BOOKS, Inc.